



End-to-end dosimetry audit for three-dimensional image-guided brachytherapy for cervical cancer

Hideyuki Mizuno^{a,*}, Taku Nakaji^a, Shigekazu Fukuda^a, Shingo Kato^b

^a Radiation quality control section, QST Hospital, National Institutes for Quantum Science and Technology, Chiba, Japan

^b Saitama Medical University International Medical Centre, Hidaka, Saitama, Japan

ARTICLE INFO

Keywords:

End-to-end
Dosimetry audit
Image-Guide brachytherapy.
Cervical cancer

ABSTRACT

Background: End-to-end dosimetry audit for brachytherapy is challenging due to the steep dose gradient. However, it is an efficient method to detect unintended errors in actual clinical practice.

Purpose: We aimed to develop an on-site end-to-end test phantom for three-dimensional image-guided brachytherapy (IGBT) for cervical cancer.

Methods: The test phantom we developed consisted of a water tank with an applicator/detector holder. The holder was designed to accommodate the applicator and insert an ionization chamber (PinPoint; PTW, Freiburg, Germany) to measure the dose at point A. Imaging and reconstruction were performed in the same way as performed for a patient. The feasibility of our test phantom was assessed in two different hospitals using tandem and ovoid (made of either metal or carbon) applicators that the hospitals provided.

Results: The measured and calculated doses at point A were compared for each applicator. We observed that the values obtained using metal applicators were consistently lower, on an average by -2.3% , than the calculated values, while those obtained using carbon applicators were comparable to the calculated values. This difference can be attributed to the attenuation of the dose by the metal applicators, resulting in a lower dose at point A. The majority of treatment planning system, including the one used in this study, do not account for the material of applicator.

Conclusions: An end-to-end test phantom for IGBT was developed, tested, and applied in a dosimetry audit in hospitals and showed favorable results for evaluating the point A dose.

1. Introduction

Radiation therapy dosimetry audits have a lengthy history, dating back to their initiation by the International Atomic Energy Agency in 1969 [1]. Several studies have reported the importance of dosimetry audits [2–5]. Previous audits in radiation therapy have mainly focused on external beam radiation therapy, with less emphasis on brachytherapy [6]. Brachytherapy dosimetry is challenging due to the steep dose gradient. Initially, brachytherapy audits were limited to source strength checks [7,8]. Subsequently, a geometric check procedure for the treatment planning system (TPS) reconstruction technique was developed [9]. These checks were simple source motion assessments rather than position checks in actual clinical situations. Therefore, there is a need for end-to-end tests for more robust dosimetry audits. Recently, the number of treatments using three-dimensional (3D)-image-guided brachytherapy (IGBT) has increased, and currently, this method is accepted as the

recommended practice in brachytherapy [10,11]. Using computed tomography (CT)/magnetic resonance imaging (MRI), the accuracy of delivering a sufficient dose to the target has significantly improved. The source dwell positions and irradiation times are adjusted based on the obtained images. Thus, dosimetry audits of the entire treatment systems, such as end-to-end tests, are necessary for modern brachytherapy. A few studies have performed end-to-end tests for brachytherapy [12,13]. The phantom used in these studies was simple and facilitated a precise comparison of the measured and calculated doses. However, the studies utilized applicators specific to their research rather than those provided by the hospitals. The applicator offset check, distance check from the applicator tip to the first source dwell position, is a critical parameter of the IGBT technique and is essential in real clinical situations, as some accidents have been attributed to this factor. Krause et al. utilized clinical applicators in their end-to-end tests [14]. However, they only used cylindrical-type applicators, which are scarcely used in cervical

* Corresponding author at: 4-9-1 Anagawa, Inage-ku, Chiba, Chiba, Japan.

E-mail address: mizuno.hideyuki@qst.go.jp (H. Mizuno).

<https://doi.org/10.1016/j.ejmp.2024.103321>

Received 16 August 2023; Received in revised form 8 February 2024; Accepted 12 February 2024

Available online 22 February 2024

1120-1797/© 2024 Associazione Italiana di Fisica Medica e Sanitaria. Published by Elsevier Ltd. All rights reserved.

a)

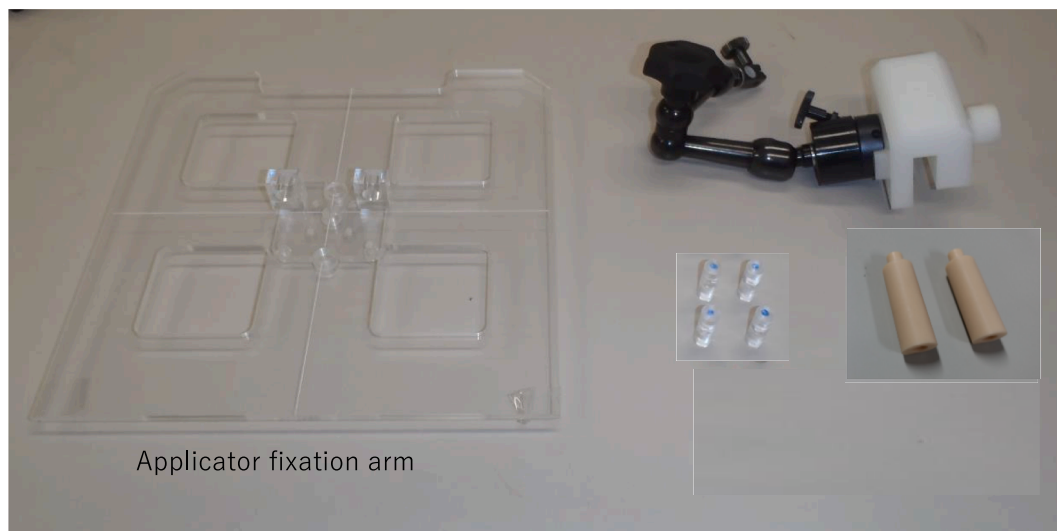


Fig. 1. Developed phantom system. (a) Applicator/detector holder, jig, and dummy detector. (b) End-to-end setting used in the phantom system (c) schematic view of the phantom.

cancer patients. Palmer et al. used a ring applicator, one of the major applicators used in cervical cancer patients [15,16] along with a Gafchromic film to measure the dose. Their study was the first to perform a practical end-to-end test. However, film analysis can take several days; hence, resolving the problem during an on-site audit is difficult. Unlike the previous study, we adopted an ionization chamber as the detector and developed an end-to-end test phantom. The results can be obtained in real time using an ionization chamber; if the results are unsatisfactory, some interventions can be performed in the hospital immediately after the irradiation session to improve the results. This study aimed to examine the developed dosimetry audit phantom for IGBT, a simple method with low cost and complexity, and determine the feasibility of actual dosimetry audits performed in hospitals.

2. Materials and methods

2.1. Specification of the phantom system

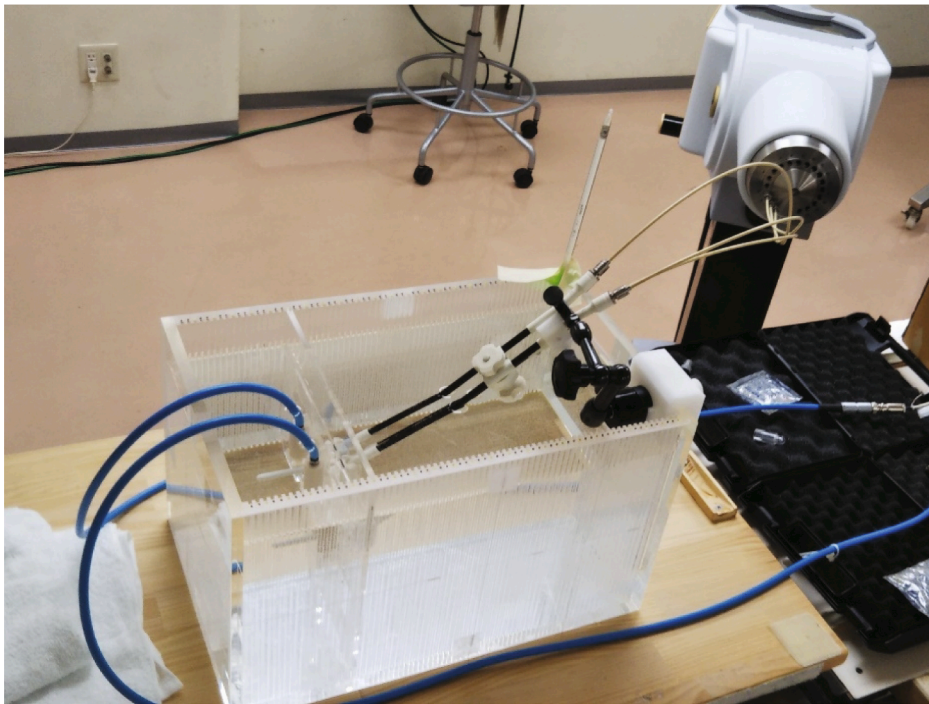
To conduct an end-to-end test, the phantom system should possess the following features: (1) usability with an appropriate applicator (such as a tandem and ovoid) and detector fixation (ideally the user's applicator), (2) suitability of the phantom to be scanned by CT and MRI images, (3) capability to detect fiducial markers on CT/MRI images to determine the effective point of measurement (EPOM), (4) construction from water or a water-equivalent material, and (5) ease of use for on-site audits. This study performed a CT image-based IGBT; therefore, several metal materials for the fixation arm were used to fix the applicator in the phantom system. All metal components should be positioned away from the region of interest in the CT image to avoid metal artifact effects. To satisfy all requirements for the phantom system, we utilized a water tank with an applicator holder, which enabled the insertion of the applicator. The use of water and the holder permits the inclusion of various applicator shapes from different manufacturers. The holder was specifically designed to secure the applicator and enable the insertion of ionization chambers or dummy detectors, fulfilling the phantom system's first, second, fourth, and fifth requirements. A dummy detector with an air hole was utilized for the third requirement, clearly visible in CT images. The position of the air hole in the dummy detector corresponds to the EPOM of the dosimeter. The dosimetric positions at right and left points

A [17] were selected for patients with cervical cancer. These positions are traditionally used for dose prescription in the treatment of cervical cancer. In addition, because dosimetry in brachytherapy is sensitive to even slight source position shifts within the applicator inner space, measuring both right and left points simultaneously can compensate for any minor dosimetry fluctuations.

2.2. Developed phantom system

The water tank was 230.6 mm (width) \times 224.0 mm (height) \times 350 mm (length) (Fig. 1). The wall of the phantom was modified with slot cuts at 5 mm intervals to allow for the insertion of the applicator holder. The holder had a central hole for tandem insertion and a groove for the ionization chamber, with a diameter of 8.1 mm. The hole is made of rubber to prevent the inserted tandem from shifting. The tandem was inserted until the tandem ring (assuming the position of the external OS of the uterus (EOS)) pressed against the holder surface. The diameter of the hole was smaller than that of the ring, and only the tandem was inserted. Therefore, the intersection of the tandem and holder surface can be assumed as the EOS, and point A is defined based on the position of the EOS. A hole was created to hold the ionization chamber to ensure that the EPOM corresponds to the position of point A. A fiducial marker with a 2-mm air hole inside was also manufactured, and the air hole corresponded to the position of point A (Fig. 2). To provide full scattering conditions, the underlying assumption of the TPS calculation was that patient size is infinite. However, the size of the water tank is finite and may underestimate the dose by measurement. According to a previous study [18], this effect was calculated to decrease the radial dose function by about 1 % at a distance of about 3 cm from the source for a spherical phantom of radius 10 cm. For a phantom with a radius of 15 cm, the radial dose function decreases by 1 % at about 5 cm. Our phantom geometry corresponds to a case with a radius between 10 and 15 cm. The main contribution to point A dose is from the nearest source at a distance of 2 cm and the contribution decreases significantly depending on source-to-chamber distance. Based on this consideration, a 1 % uncertainty was added to the uncertainty budget.

b)



c)

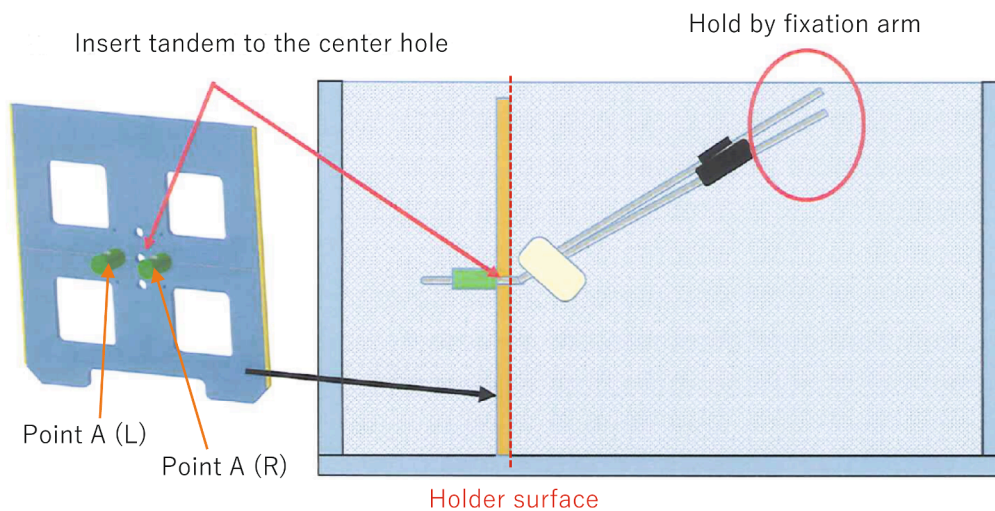


Fig. 1. (continued).

2.3. Dosimeter

A PinPoint ionization chamber (TN31014; PTW, Freiburg, Germany) in combination with a PC electrometer (Sun Nuclear) was used as the dosimeter to measure the point A dose. The PC electrometer used in this study is equipped with two channels, allowing for the simultaneous measurement of left and right doses at point A during a single-fraction dose delivery using two PinPoint chambers. To ensure accurate measurements, the dosimeter was calibrated by the Secondary Standard Dosimetry Laboratories in Japan using Cobalt-60 gamma rays. The Japan Society of Medical Physics' Standard Dosimetry in Brachytherapy 18 [19] was used as the dosimetry protocol. The absorbed dose is

expressed as the following equation in the protocol.

$$D_w = MN_{D,w}^{Co60} k_{Ir}$$

where M is the reading of the dosimeter under the user radiation quality and $N_{D,w}^{Co60}$ is the calibration factor in terms of absorbed dose to water of the dosimeter obtained from a standards laboratory and the factor k_{Ir} corrects for the effects of the difference between the reference beam quality from ^{60}Co -gamma ray and the actual user quality from ^{192}Ir -gamma ray. However, only the k_{Ir} for Farmer-type chamber is given in the protocol. The quality conversion factor of the Farmer-type chamber changes significantly around 2 cm to 4 cm, mostly by volume averaging

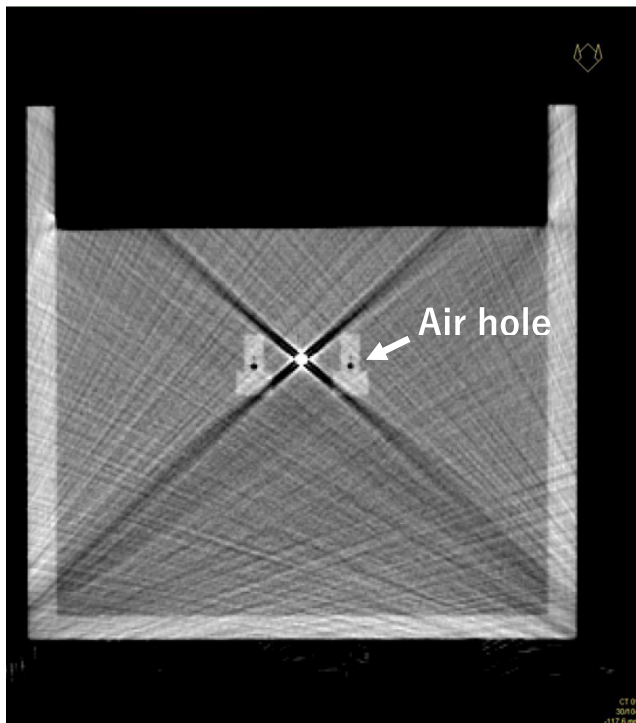


Fig. 2. Computed tomography images of the phantom. Despite the appearance of the metal artifacts from the applicator, air holes were visualized in the axial plane. The hole corresponds to point A (left and right) and indicates the EPOM of the PinPoint chamber.

effect. The small volume chamber is suitable for dosimetry at distances only a few cm from the radiation source. Therefore, we chose the PinPoint for this study. Unfortunately, no reliable data are available for the k_{tr} of PinPoint. Candela et al. used a beam quality correction factor of 1.0 for the PinPoint ionization chamber (PTW T31016) and assumed the maximum effect of the correction factor to be 1.8 % [20]. The nominal sensitive volume between the two types is almost the same (0.015 cm³ for T31014 and 0.016 cm³ for T31016). However, the dimension of the sensitive volume was not equal (radius 1 mm, length 5 mm for T31014 and radius 1.45 mm, length 2.9 mm for T31016). We decided to direct the shorter axis to the largest gradient direction, perpendicular to the

tandem axis. Considering this, we initially assumed a correction factor of 1.0 and expected a corresponding uncertainty of 1.8 % in the output.

2.4. Feasibility end-to-end test

An end-to-end feasibility test was conducted at QST Hospital and Saitama Medical University International Medical Centre (SMUIMC). The end-to-end test of the IGBT was performed based on the following steps:

1. Applicator was installed to the phantom via the applicator holder with fixtures.
2. Dummy detectors were placed in the ionization chamber holder.
3. CT images were acquired using the same protocol (field of view, slice thickness, etc.) as used in patients with cervical cancer.
4. The applicator reconstruction was performed in the same manner as that used in patients in clinical practice and a standard plan was used. The dwell time weights for each source position were set equal except at the tandem tip as is the usual protocol in clinical practice (half the weight is assigned to the tip). At point A, the prescribed dose was the same as the regular dose (e.g., 6 Gy). The air hole in the dummy detector was assigned as the TPS dosimetry point, and the dose was evaluated.
5. The phantom was placed in the brachytherapy treatment room, and the dummy detectors were replaced with PinPoint chambers.

Irradiation was performed according to the treatment plan, and the dose was measured using a PinPoint chamber. The measured values were compared with the calculated values. Irradiation was performed thrice, and the results were averaged.

Feasibility measurements were performed using two different applicators at QST hospital. One applicator was a metal (Fletcher Williamson Asia Pacific Set (#085.260), Nucletron B.V.), while the other was a carbon (Standard CT/MR Applicator Set (#101.020), Nucletron B. V.), which is MRI compatible. The calculation algorithm is AAPM TG-43 [21], which does not take correction factors into account for applicator material.

The brachytherapy system used in SMUIMC was a microSelectron HDR, and the TPS used was Oncentra. The radiation source was ¹⁹²Ir, and the applicator was made of metal. The time required for the end-to-end test was at least three hours. Installation of an applicator in this phantom system is somewhat difficult and requires assistant from

Table 1

Dose measured and calculated for the feasibility end-to-end test. The measured and calculated doses of each applicator irradiation delivered to point A (R) and point A (L) positions were compared. < metal > represents the results of the metal applicator, while < carbon > represents the results of the carbon applicator.

Measured position	Point A (R)	Point A (L)	Point A (R)	Point A (L)	Point A (R)	Point A (L)	Point A (R)	Point A (L)
Irradiated Applicator	Ovoid (R)	Ovoid (R)	Ovoid (L)	Ovoid (L)	Tandem	Tandem	Ovoid +Tandem (R)	Ovoid +Tandem (L)
<metal> Measured Dose [Gy]	1.26	0.69	0.69	1.47	3.89	3.40	5.84	5.56
<metal> Calculated Dose [Gy]	1.32	0.728	0.68	1.43	3.84	3.67	5.84	5.83
<metal> Measured /calculated	-4.4 %	-4.9 %	+1.2 %	+2.5 %	+1.2 %	-7.4 %	0.0 %	-4.6 %
<carbon> Measured dose [Gy]	1.39	0.79	0.80	1.38	3.87	3.65	6.06	5.83
<carbon> Calculated dose [Gy]	1.33	0.77	0.79	1.34	3.84	3.75	5.96	5.85
<carbon> Measured /calculated	+4.3 %	+3.5 %	+2.3 %	+3.5 %	+0.8 %	-2.5 %	+1.8 %	-0.3 %

(a)

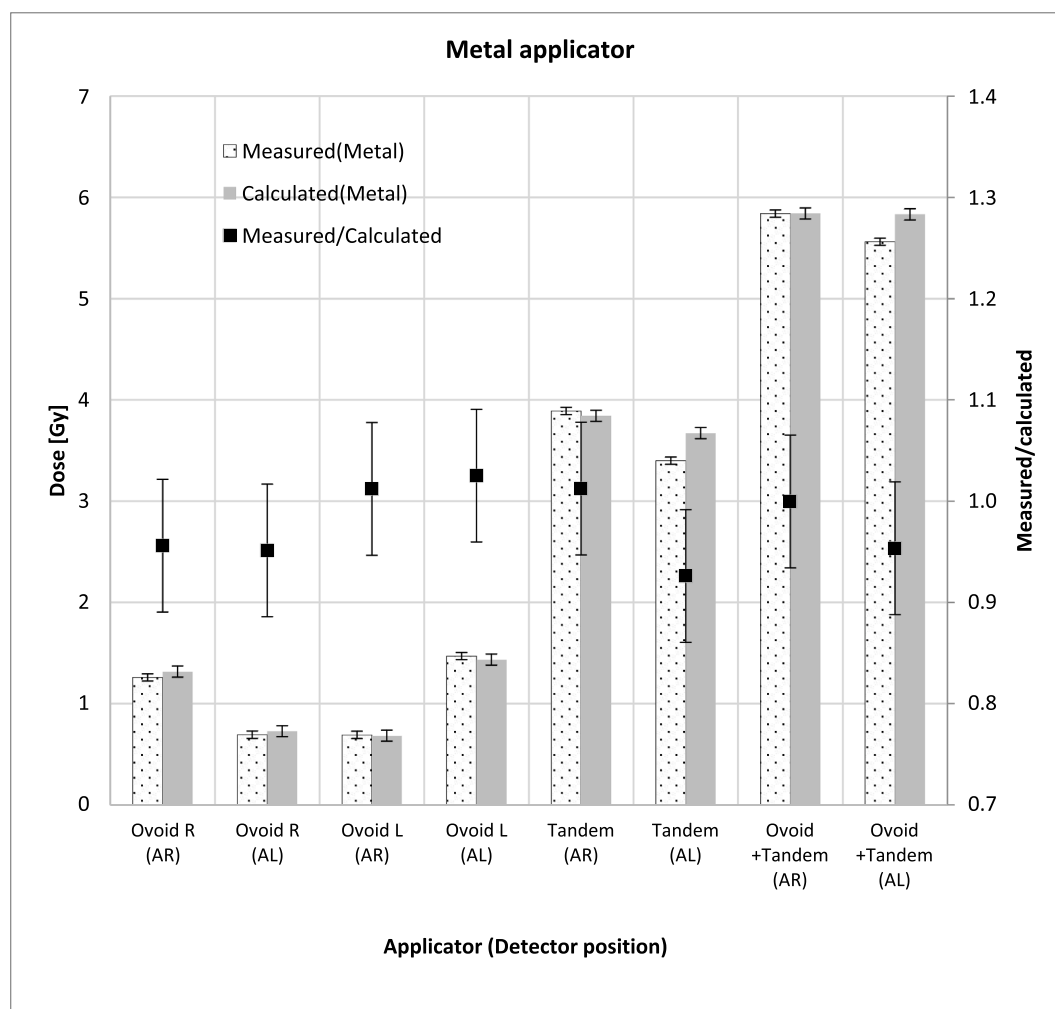


Fig. 3. (a) Measured and calculated doses to point As of the metal applicator. (b) Measured and calculated doses to point As of the carbon applicator. The doses were indicated separately for each applicator channel (ovoid R, ovoid L, and tandem). The measured dose-to-calculated dose ratio is also plotted using a second vertical axis. The error bar of measured data is taken from the uncertainty budget (Table 3) of PinPoint chamber dosimetry.

experienced staff. However, the workflow is the same as that in clinical practice.

3. Results

The feasibility of the end-to-end test at the QST hospital is demonstrated in Table 1 and Fig. 3 (a) and (b). The measured and calculated doses for each applicator irradiation delivered to point A's left and right sides were compared. The ratio of the measured and calculated doses was within 5 %, except for one condition where tandem irradiation was performed at point A (L).

The results of the feasibility end-to-end test performed for the SMUIMC are shown in Table 2 and Fig. 4. Similarly, good results were obtained, that is, the difference ratio between the measured and calculated values was within 4 % on the right and left sides of point A, except for one condition which underwent ovoid (L) irradiation at point A (R).

In all cases, applicator reconstruction was assessed by checking the TPS display for agreement between reconstructed applicator outline and the actual applicator shape on the CT image. In addition, the calculation point (point A) was shifted by 0.5 mm in all 3-D directions to evaluate the effect of positional uncertainty. The evaluation assumes applicator

movement, or source position within the applicator, or reproducibility of source position. The dose difference results for offset positions from the original position ranged from -2.6% to $+2.7\%$ (rounded to $\pm 3\%$). The steepest descent direction was conservatively chosen to derive positional uncertainty.

4. Discussion

The estimated uncertainty, including the PinPoint dosimetry, is summarized in Table 3. According to the American Association of Physicists in Medicine and Groupe Européen de Curiethérapie and the European Society for Radiotherapy & Oncology guidelines [22], the dosimetric uncertainty rates for the HDR ^{192}Ir source for intracavitary IGBT were as follows: source strength: 2 %, treatment planning: 3 %, medium dosimetric corrections: 1 %, and dose delivery including registration of applicator geometry to anatomy: 4 %. The uncertainty of the PinPoint dosimetry is determined by several factors, including the calibration uncertainty referenced from the calibration certificate, the chamber position derived from the 0.5 mm shift of the dose distribution calculated by the TPS, and the measurement stability derived from the PinPoint output reproducibility. The combined uncertainty, 6.6 %, was

(b)

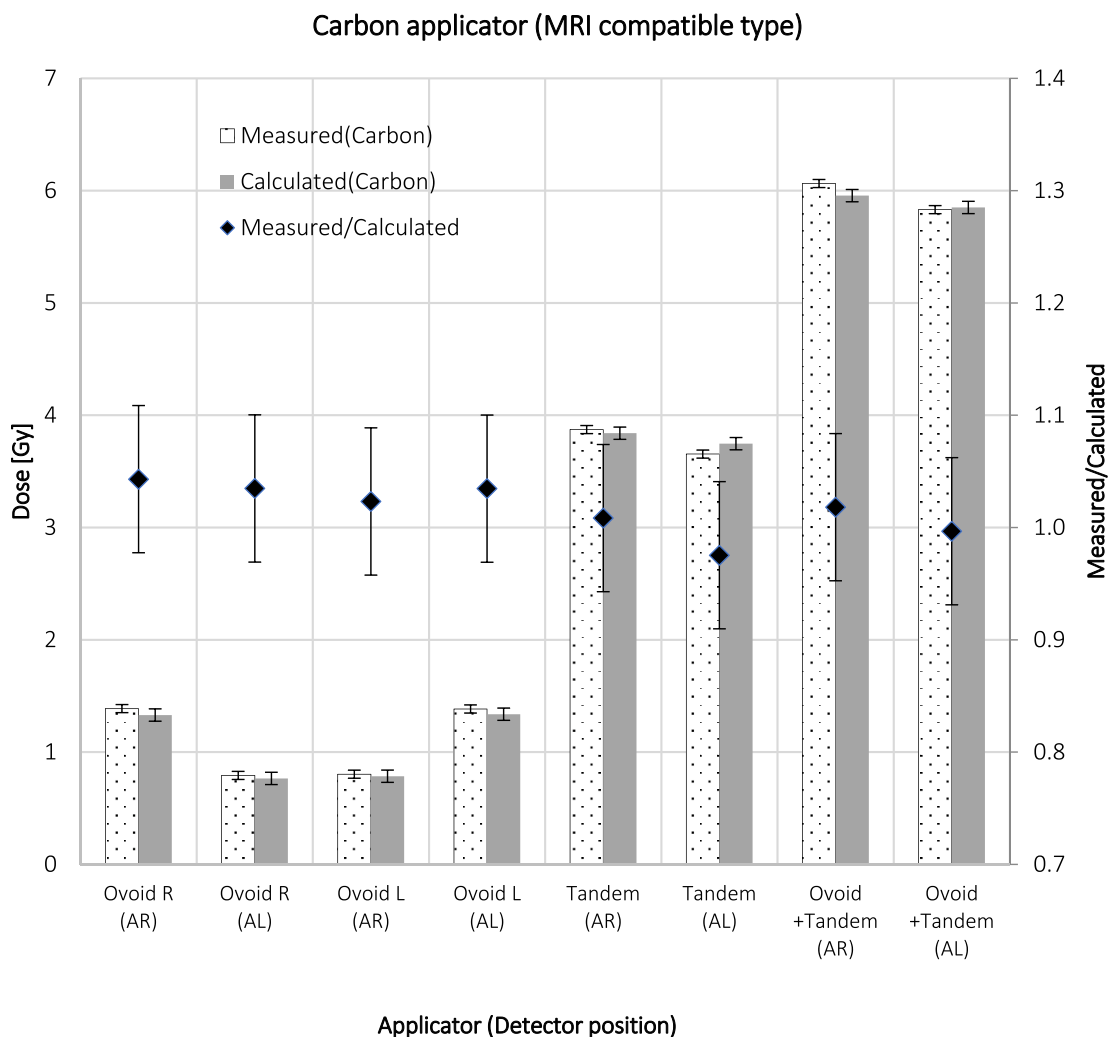


Fig. 3. (continued).

Table 2

Measured and calculated doses for the feasibility end-to-end test at SMUIMC. The measured and calculated doses of each applicator irradiation delivered at point A (R) and point A (L) positions were compared. SMUIMC, Saitama Medical University International Medical Centre.

Measured position	Point A (R)	Point A (L)	Point A (R)	Point A (L)	Point A (R)	Point A (L)	Point A (R)	Point A (L)
Irradiated Applicator	Ovoid (R)	Ovoid (R)	Ovoid (L)	Ovoid (L)	Tandem	Tandem	Ovoid +Tandem	Ovoid +Tandem
<metal> Measured Dose [Gy]	0.80	0.38	0.39	0.85	4.27	4.16	5.46	5.39
<metal> Calculated Dose [Gy]	0.83	0.39	0.41	0.85	4.41	4.28	5.65	5.52
<metal> Measured /Calculated	-3.0 %	-2.4 %	-5.5 %	-0.2 %	-3.2 %	-2.7 %	-3.3 %	-2.3 %

considered the inspection level. In addition, doubled value, 13.3 %, was considered immediate action level. The action level of ± 13.3 % appears to be larger than the 10 % level, which is sometimes referred to as clinically relevant error. The tolerance level may be based not only on the performance of the measurement system, but also on the judgement of clinical acceptability. The value of 10 % is between the inspection level and the immediate action level. From this point of view, it is

preferable to assess the measurement results with emphasis on 6.6 % of the inspection level. Considering this level, the results of this feasibility study seemed to be satisfactory in assessing the accuracy of dose prescription.

Analysis of the comparative data for each applicator revealed a dependence on the material of the applicator. Specifically, when metal, stainless steel, applicators were used at the QST hospital and SMUIMC,

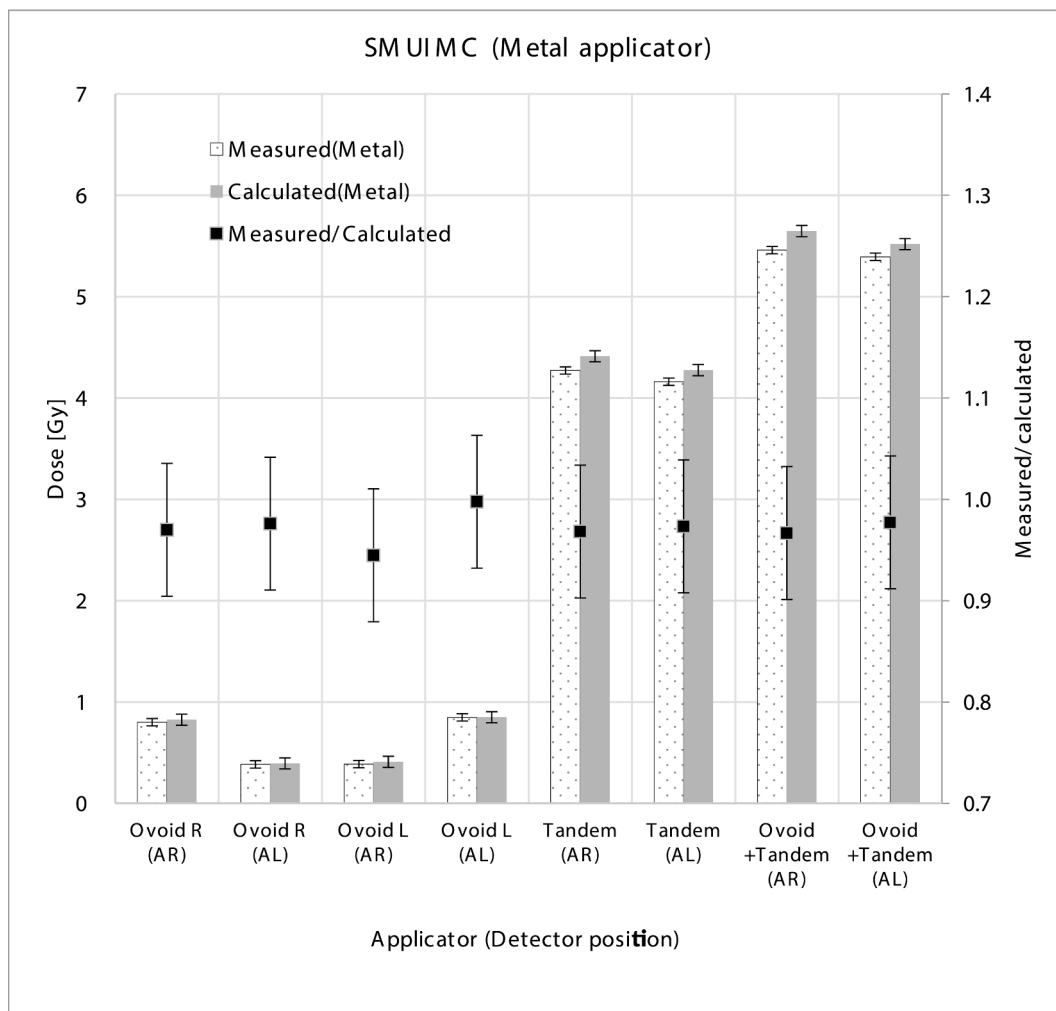


Fig. 4. Measured and calculated doses to point As for the SMUIMC (using a metal applicator). The doses were indicated separately for each applicator channel (ovoid R, ovoid L, and tandem). The percentage ratio of the measured dose to the calculated dose is also plotted using a second vertical axis. The error bar of measured data is taken from the uncertainty budget (Table 3) of PinPoint chamber dosimetry.

Table 3

Uncertainty budget for the experimental determination of the agreement between TPS planned and EtoE phantom measured dose by PinPoint chamber at Point A.

Category	Type	Uncertainty [%] (k = 1)
Source strength [22]	B	2
Treatment planning [22]	B	3
Medium dosimetric corrections [22]	B	1
Dose delivery including registration of applicator geometry to anatomy [22]	B	4
Phantom size correction	B	1
PinPoint dosimetry;		
Calibration	B	0.7
Chamber position	B	3
Beam quality correction factor	B	1.8
Measurement stability	A	0.7
Combined uncertainty		6.6
Expanded uncertainty (k = 2)		13.3

the measured values were systematically lower than the calculated values. The average percentage difference in dose for all applicators was - 2.3 %. By contrast, the measured doses were systematically higher than those calculated for the carbon applicator. The average percentage

difference in the dose difference for all applicators was + 0.7 %. The metal attenuated the dose, reducing the dose at point A. Palmer et al. reported that in 46 audited brachytherapy centers, the differences between the measured and calculated doses at point A for metal and plastic applicators were -3.0 % and -0.6 %, respectively [16]. This difference is consistent with our results. Some types of TPS (The Eckert & Ziegler Bebig GmbH SagiPlan and HDRPlus) include automatic correction of metal applicator attenuation; another type (Elekta Oncentra) only provides an option for correction (F-Factor). However, these methods have not been widely implemented. The TPS used in this study did not include such automatic correction.

Finally, it is important to outline the steps to take in case of any discrepancies found in the dosimetry results using this methodology. The course of action would depend on the nature of the discrepancy. For instance, a source strength check should be performed if the measured dose is consistently different from the calculated dose. This can begin with a consistency check using source specification data, and TPS installed data, followed by well-type chamber measurement. For example, if the dosimetry results are unbalanced on the right and left sides, applicator position reproducibility should be examined. Using the phantom eliminates exposure limitations and allows for multiple CT acquisitions, even after brachytherapy irradiation. If the source position is determined to be accurate, attention should be directed towards the applicator offset—the distance between the applicator tip and the first

source dwell position—as this is a critical parameter in IGBT practice. For some TPS, the offset value must be manually inputted for each plan, which could lead to typographical errors. The applicator offset value can be easily measured using film.

5. Conclusion

To summarize, a dosimetry test object for IGBT was developed, tested, and applied in hospital dosimetry audits. The system performed effectively, successfully measuring the dose to point. The use of PinPoint chamber resulted in an estimated uncertainty of $\pm 6.6\%$ in one standard deviation. End-to-end dosimetry audits for modern techniques such as IGBT have not yet been established worldwide. This activity is one of the most practical trials in an IGBT audit.

Declarations.

Funding: This work was supported by JSPS KAKENHI Grant Number 17 K09075.

Conflict of interest: All authors declare no conflicts of interest.

Ethics approval: This study did not involve any human participants or animals.

CRediT authorship contribution statement

Hideyuki Mizuno: Conceptualization, Investigation, Methodology, Project administration, Writing original draft. **Taku Nakaji:** Investigation, Methodology. **Shigekazu Fukuda:** Review & editing. **Shingo Kato:** Review & editing.

Declaration of competing interest

The authors declare that they have no known competing financial interests or personal relationships that could have appeared to influence the work reported in this paper.

Acknowledgments:

This work was supported by JSPS KAKENHI Grant Number 17 K09075.

References

- [1] Izewska J, Andreo P. The IAEA/WHO TLD postal programme for radiotherapy hospitals. *Radiother Oncol* 2000;54:65–72. [https://doi.org/10.1016/s0167-8140\(99\)00164-4](https://doi.org/10.1016/s0167-8140(99)00164-4).
- [2] Izewska J, Lechner W, Wesolowska P. Global availability of dosimetry audits in radiotherapy: The IAEA dosimetry audit networks database. *Phys Imaging Radiat Oncol* 2018;5:1–4. <https://doi.org/10.1016/j.phro.2017.12.002>.
- [3] Kry SF, Peterson CB, Howell RM, Izewska J, Lye J, Clark CH, et al. Remote beam output audits: a global assessment of results out of tolerance. *Phys Imaging Radiat Oncol* 2018;7:39–44. <https://doi.org/10.1016/j.phro.2018.01.002>.
- [4] Mizuno H, Fukumura A, Fukahori M, Sakata S, Yamashita W, Takase N, et al. Application of a radiophotoluminescent glass dosimeter to nonreference condition dosimetry in the postal dose audit system. *Med Phys* 2014;41:112104. <https://doi.org/10.1118/1.4898596>.
- [5] Mizuno H, Yamashita W, Okuyama H, Takase N, Tohyama N, Shimizu H, et al. Dose response of a radiophotoluminescent glass dosimeter for TomoTherapy, CyberKnife, and flattening-filter-free linear accelerator output measurements in dosimetry audit. *Phys Med* 2021;88:91–7. <https://doi.org/10.1016/j.ejmp.2021.06.010>.
- [6] Palmer AL, Bradley DA, Nisbet A. Dosimetric audit in brachytherapy. *Br J Radiol* 2014;87:20140506. <https://doi.org/10.1259/bjr.20140105>.
- [7] Venselaar JLM, Brouwer WFM, van Straaten BHM, Aalbers AHL. Intercomparison of calibration procedures for Ir-192 HDR sources in the Netherlands and Belgium. *Radiother Oncol* 1994;30:155–61. [https://doi.org/10.1016/0167-8140\(94\)90046-9](https://doi.org/10.1016/0167-8140(94)90046-9).
- [8] de Almeida CE, Pereira AJ, Marechal MH, Pereira G, Cruz JC, Ferraz JC, et al. Intercomparison of calibration procedures for 192Ir HDR sources in Brazil. *Phys Med Biol* 1999;44:N31–8. <https://doi.org/10.1088/0031-9155/44/3/006>.
- [9] Roué A, Ferreira IH, Van Dam J, Svensson H, Venselaar JL. The EQUAL-ESTRO audit on geometric reconstruction techniques in brachytherapy. *Radiother Oncol* 2006;78:78–83. <https://doi.org/10.1016/j.radonc.2005.12.004>.
- [10] Haie-Meder C, Pötter R, Van Limbergen E, Briot E, De Brabandere M, Dimopoulos J, et al. Recommendations from Gynaecological (GYN) GEC-ESTRO Working Group (I): concepts and terms in 3D image based 3D treatment planning in cervix cancer brachytherapy with emphasis on MRI assessment of GTV and CTV. *Radiother Oncol* 2005;74:235–45. <https://doi.org/10.1016/j.radonc.2004.12.015>.
- [11] Pötter R, Haie-Meder C, Van Limbergen E, Barillot I, De Brabandere M, Dimopoulos J, et al. Recommendations from Gynecological (GYN) GEC ESTRO working group (II): concepts and terms in 3D image-based treatment planning in cervix cancer brachytherapy—3D dose volume parameters and aspects of 3D image-based anatomy, radiation physics, radiobiology. *Radiother Oncol* 2006;78: 67–77. <https://doi.org/10.1016/j.radonc.2005.11.014>.
- [12] Haworth A, Wilfert L, Butler D, Ebert MA, Todd S, Bucci J, et al. Australasian brachytherapy audit: results of the “end-to-end” dosimetry pilot study. *J Med Imag Radiat Oncol* 2013;57:490–8. <https://doi.org/10.1111/1754-9485.12042>.
- [13] Bassi S, Berrigan L, Zuchora A, Fahy L, Moore M. End-to-end dosimetric audit: a novel procedure developed for Irish HDR brachytherapy centres. *Phys Med* 2020; 80:221–9. <https://doi.org/10.1016/j.ejmp.2020.10.005>.
- [14] Krause F, Risske F, Bohn S, Delaperriere M, Dunst J, Siebert FA. End-to-end test for computed tomography-based high-dose-rate brachytherapy. *J Contemp Brachytherapy* 2018;10:551–8. <https://doi.org/10.5114/jcb.2018.81026>.
- [15] Palmer AL, Lee C, Ratcliffe AJ, Bradley D, Nisbet A. Design and implementation of a film dosimetry audit tool for comparison of planned and delivered dose distributions in high dose rate (HDR) brachytherapy. *Phys Med Biol* 2013;58: 6623–40. <https://doi.org/10.1088/0031-9155/58/19/6623>.
- [16] Palmer AL, Diez P, Gandon L, Wynn-Jones A, Bownes P, Lee C, et al. A multicentre “end to end” dosimetry audit for cervix HDR brachytherapy treatment. *Radiother Oncol* 2015;114:264–71. <https://doi.org/10.1016/j.radonc.2015.03.024>.
- [17] International commission on radiation units and measurements. ICRU report No. 89: prescribing, recording, and reporting brachytherapy for cancer of the cervix. *J ICRU* 2013;13:1–2.NP. <https://doi.org/10.1093/jicru/ndw027>.
- [18] Pérez-Calatayud J, Granero D, Ballester F. *Med Phys* 2004;31(7):2075–81. <https://doi.org/10.1118/1.1759826>.
- [19] *Japan Society of Medical Physics. Standard Dosimetry in Brachytherapy 18. Tokyo: Tsusho-sangyo-kenkyusya; 2018. in Japanese.*
- [20] Candela-Juan C, Niatsetski Y, van der Laarse R, Granero D, Ballester F, Perez-Calatayud J, et al. Design and characterization of a new high-dose-rate brachytherapy Valencia applicator for larger skin lesions. *Med Phys* 2016;43:1639. <https://doi.org/10.1118/1.4943381>.
- [21] Nath R, Anderson LL, Luxton G, Weaver KA, Williamson JF, Meigooni AS. Dosimetry of interstitial brachytherapy sources: recommendations of the AAPM radiation therapy committee task group no 43. *Med Phys* 1995;22(2):209–34. <https://doi.org/10.1118/1.597458>.
- [22] Kirisits C, Rivard MJ, Baltas D, Ballester F, De Brabandere M, van der Laarse R, et al. Review of clinical brachytherapy uncertainties: analysis guidelines of GEC-ESTRO and the AAPM. *Radiother Oncol* 2014;110:199–212. <https://doi.org/10.1016/j.radonc.2013.11.002>.